Tunable from blue to red emissive composites and solids of silver diphosphane systems with higher quantum yields than the diphosphane ligands

María Calvo[a], Olga Crespo[a]*, M. Concepción Gimeno[a]*, Antonio Laguna[a], M. Teresa Oliván[a], Víctor Polo[b], Diego Rodríguez[a], Jose-M. Sáez-Rocher[a]

[a]Departamento de Química Inorgánica, Instituto de Síntesis Química y Catálisis Homogénea (ISQCH). Universidad de Zaragoza-CSIC. E-50009 Zaragoza, Spain.

[b]Departamento de Química Física, Instituto de Biocomputación y física de Sistemas Complejos (BIFI). Universidad de Zaragoza, Facutad de Ciencias E-50009 Zaragoza, Spain

KEYWORDS: Luminescence, TADF, Silver, Film composites, Quantum Yield, Theoretical studies, Carborane, Diphosphane

ABSTRACT: PMMA composites and solids of complexes of formulae [AgX(P-P)]n [n = 1, 2; X = Cl, NO3, ClO4, CF3COO, OTf; P-P = dppb, xantphos, (PR2)2C2B10H10 (R = Ph, ^{i}Pr)] display the whole palette of colors, from blue to red upon selection of the anionic ligand (X) and the diphosphane (P-P). The diphosphane seems to play the most important role in tuning the emission energy and TADF behavior. The PMMA composites of the complexes exhibit higher quantum yields than that of the diphosphane ligands and those with dppb are between 28 and 53%. Remarkably, instead of blue-green emissions, which dominate the luminescence of silver diphosphane complexes in rigid phases, those with carborane diphosphanes are yellow-orange or orange-red emitters. Theoretical studies have been carried out for complexes with P-P = dppb, X = Cl), P-P = dppic, X = NO_3, P-P = dppcc, X = Cl, NO_3, OTf and the mononuclear complexes [AgX(xantphos)] (X = Cl, Br). Optimization of the first excited triplet state was only possible for [AgX(xantphos)] (X = Cl, Br). A mixed MLCT and MC nature could be attributed to the $S_0 \leftarrow T_1$ transition in these three coordinated complexes.

INTRODUCTION

Some silver tetracoordinated diphosphane complexes in which the diphosphane acts in a chelate mode show interesting emissive behaviors as thermally activated delayed fluorescence (TADF[1], reported as a rapid process to harvest 75% of triplet excitons for luminescence, which represents an advantage in the design of OLEDs) or mechanochromism. These findings have prompted us to analyze the related literature with the aim of searching for general emissive trends.

Luminescent homoleptic $[Ag(P\text{-}P)_2]X$ complexes [X = BF_4 or NO_3; P-P = diphosphane], as a general tendency, display blue emissions in solid state and rigid THF or MeOH/EtOH (4:1) matrix, although red emissions have been reported in solution. From DFT studies the red emissions have been related with a ^{3}MC excited state, based on square-planar geometry at silver. The blue emissions have been attributed to ^{3}MLCT excited state based on tetrahedral geometry.[2-3] Blue-green emissive character may be extended to *heteroleptic species*[4-14] despite their structures and auxiliary ligands. Thus, it has been observed for mononuclear [Ag(P-P)L] (L = any bidentate chelate ligand) and dinuclear $[AgX(P\text{-}P)]_2$ (X = thiolate, thiocyanate or bromide)[9,10,15] species, but also in more complicated structures, as silver compounds with the diphosphane in a bridging mode instead of a chelate one[8]; in complexes with N donor auxiliary ligands[11,12] (which display ring chains or network structures) and in alkynyl derivatives of stoichiometry $[Ag_3\{\mu\text{-}(P\text{-}P)\}_3\{\mu_3\eta^1\text{-}C{\equiv}CR\}]$[13]. Even three coordinated carbene complexes[14] display this trend showing emissions from blue to yellow.

Although still scarcely represented, it is growing the number of silver derivatives for which TADF is proposed, and in some cases lifetimes of the singlet and triplet state and the corresponding $\Delta E(S_1\text{-}T_1)$ energy gap are reported.[5,10,15-22]. Mechanochromism, from blue to green, has been reported[6] for $[Ag(dppb)(dppaS_2^-)]$ ($dppaS_2^-$ = imidotetraphenyldithiodiphosphinate) and $[Ag(SCN)P^4]$ (P^4 = tris(2-diphenylphoshino)phenylphosphine).[15] Fabrication and characterization of an emitting device which produces almost white light with $[Ag(dppb)_2]BF_4$ has been reported.[2]

The analysis of the above mentioned examples indicates that, despite the diphosphane coordination mode and the

complexity of the structure, silver diphosphane compounds display mainly blue-green emission in rigid media (in the solid state or cold rigid solvent matrix). Thus, modulation of the emissions in order to cover the whole visible spectrum and experimental information of the ligands which favor TADF may be considered goals for this topic.

With these questions in mind we present a comparative study involving silver complexes combining diphosphanes and different anions (halogens or pseudohalogens) taking into account that, despite of the established synthetic procedures and structural features, the emissive properties of $[AgX(P\text{-}P)]_2$ (X = bridging halogen or pseudohalogen ligand) complexes have been scarcely analyzed. We have synthesized four families of complexes. Each family combines the same diphosphane with five different anionic auxiliary ligands, with the aim of analyzing the role of both, the diphosphane and the anionic ligand, in the emissive properties, including TADF behavior. In order to discuss the possible origin of the luminescence, theoretical calculations have been carried out. The comparative study is completed with the analysis of the data corresponding to similar reported complexes.

Thinking in the study of emissive properties of complexes to be applied in the design of different devices, the emissive properties of films would better resemble those in the devices. This fact prompts the number of studies focused on the luminescence of films of silver complexes to increase. In these sense we have included the photoluminescence behavior of composites of the complexes in PMMA

DISCUSSION

Synthesis and characterization

Reaction of the silver salt AgX with the corresponding diphosphane, in dichloromethane or dichloromethane/diethyl ether mixtures, leads to complexes $[AgX(P\text{-}P)]_n$ (P-P = diphosphane, n = 1,2) (Scheme 1, see experimental part for synthesis and characterization details).

Crystal structures of complexes **1** and **17** have been elucidated by X-ray studies (Figure 1). The observed arrangement is widely represented in silver chemistry (see further discussion in S.I.) and consists in dinuclear units in which each silver atom is coordinated to a diphosphane in a chelate mode. The two silver centers are bridged by two anions (X) and display a distorted tetrahedral environment. In complex **17** the nitrate ligands act in a monodentate mode. Analysis of geometries found for similar complexes is included in S.I. and selected distances and angles have been resumed in Table S2, which shows that for these complexes, silver···silver interactions, considered when Ag···Ag distance is less than 3.44 Å,[23] have been observed only in compounds with chloride a bridging ligand and in $[AgBr(dppb)]_2$. Thus, these interactions do not govern the formation of the dinuclear units.

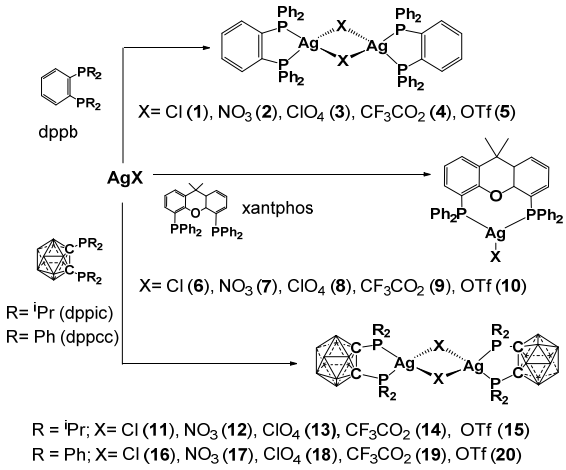

Scheme 1. Synthesis of the silver diphosphane complexes. In the dppic and dppcc diphosphanes each icosahedral vertex corresponds to a BH unit

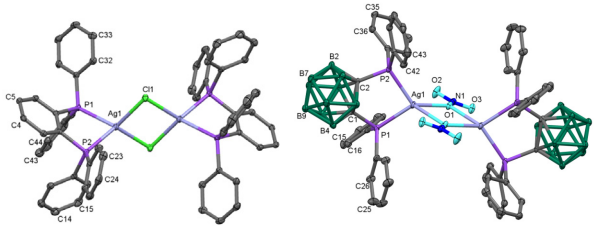

a) b)

Figure 1. Ortep diagrams of complexes **1** (a) and **17** (b). Ellipsoids are represented at 50% probability level. Hydrogen atoms have been omitted for the sake of clarity.

Emissive properties

Although emissive data for the free diphosphanes, that is, the diphosphane ligands dppb, xantphos, dppcc and dppic have been reported, we have studied their emissive behavior only for comparative purposes (Figures S3-S10, Table S3, and references therein) in the same conditions than those used for the study of complexes **1-20**. At room temperature, powder samples of carborane diphosphanes are very weekly blue emissive and PMMA films show no emission. At 77 K dual emission has been observed. The other diphosphanes (dppb and xantphos) are emissive at room temperature and 77 K. Dual emission is displayed by xantphos.

The luminescence of complexes **1-20** has been studied in the solid state for powder samples, both at room temperature and 77 K. PMMA films of **1-5** and **11-20** have also been studied at room temperature, including their quantum yields. Thus, we will analyze the influence of silver coordination and that of the change of the bridging ligand (X) and the diphosphane in the emissive properties. In addition, the effect of temperature and solid form (powder or film) changes will be studied.

Luminescence of powder samples of the silver complexes

Coordination to silver and influence of the diphosphane: Coordination of the diphosphanes to silver leads to important changes in the emissive properties, compared with that of the no coordinated carborane diphosphanes and xantphos (Tables 1 and 2, Figures 2, S11-S13). Complexes with xantphos are luminescent in the solid state at 77 K in the blue-green region and not emissive at room temperature, whereas the xantphos ligand is emissive both at room temperature and 77 K in the same region.

Table 1. Optical measurements for complexes 1-10

P-P / X (compound)		Room T.		τ(μs)[b]	Φ_{PL}(%)[c]	K_r[d]	K_{nr}[d]	77 K	
		λEx[a]	λEm[a]	(Goodness of fit)				λEx[a]	λEm[a]
dppb / Cl (**1**)	powder	386	477	14 (1.042)				*362[e], 382	466, 509
	film	300,370(sh)	515	35 (0.999)	47	$1.3\ 10^4$	$1.5\ 10^4$		
dppb / NO_3 (**2**)	powder	300	476	8.7 (1.072)				303 (br), 337	448, 478
	film	301	482	21 (0.989)	24	$1.1\ 10^4$	$3.6\ 10^4$		
dppb / ClO_4 (**3**)	powder	349	499	6 (1.026)				*314[e], 340(sh)	468, 533
	film	295	492	63 (0.998)	44	$7.0\ 10^4$	$8.8\ 10^4$		
dppb/ CF_3COO (4)	powder	346	477	7 (1.005)	13	$1.9\ 10^4$	$1.2\ 10^5$	*333[e]	467
	film	-375	496	61 (0.983)	53	8.710^3	$7.7\ 10^3$		
dppb / CF_3SO_3 (**5**)	powder	361	483	10 (1.110)				*360[e]	465
	film	282, 324	500	41 (0.997)	28	$6.8\ 10^3$	$1.8\ 10^4$		
xantphos / Cl (**6**)	powder			3776 (0.991)				320, 330	427, 521(sh)
xantphos / NO_3 (**7**)	powder			1876 (0.996)				*310[e]	417
xantphos / ClO_4 (**8**)	Powder			5044 (0.997)				*309[e]	460
xantphos / CF_3COO (**9**)	Powder			3600 (0.998)				309	423
xantphos / CF_3SO_3 (**10**)	powder			4436 (0.987)				*316[e], 350	451, 491[f]

sh = shoulder. [a]λEm = emission maximum, λEx = excitation maximum in nm. [b]Lifetimes at room temperature for complexes **1-5** and at 77 K for complexes **6-10**, see also Figures S14, S15 and Table S5. [c]Quantum yield at room temperature. [d]From the data at room temperature: calculated radiative constant $k_r = \Phi/\tau$, calculated no radiative constant $k_{nr} = (1-\Phi)/\tau$. [e]Asterisk (*) before an excitation wavelength means that the band displays maximum values from the beginning of the spectrum until this wavelength. [f]Very week band.

The silver compounds with the weak blue emissive carborane diphosphanes (**11-20**) are luminescent, both at room temperature and 77 K in the red region, although emissions at 77 K are very weak.

Complexes with the dppb ligand are blue emitters as the dppb diphosphane (Table 1). We have observed that the emissive behavior of compound **5** changes upon grinding. Figures S16 and S17 show the color change and the emission spectra, respectively. Disruption of intermolecular interactions between phenylene rings of adjacent molecules has been claimed as the origin of the emission change from blue to green upon grinding in [Ag(dppb)(dppaS_2-)].[6]

Influence of the bridging anionic ligand (X) in the emission energy does not follow a clear trend. As an example, from complexes with dppb (**1-5**) at room temperature, compound **3** (X = ClO_4) displays the lower emission energy, whereas from complexes with dppic (**11-15**), compound **13** (X = ClO4) displays the highest energy. We can conclude that it is not possible to predict the emission energy order for a family of complexes with one diphosphane attending to the anionic ligand by knowing that of the series with another diphosphane. This is consistent with the theoretical studies (see below) as orbitals of the bridging ligand do almost not contribute to the frontier orbitals.

Temperature influence: Blue and red shifts upon cooling at 77K are observed for solid samples of complexes **1-5**, **11-20**. Blue shift attributed to increment of rigidity has been reported for other complexes, although in solution media red shift was observed upon cooling, a typical behavior of complexes with small S_1-T_1 gap, revealing than rigidochromic effects may prevail or not over electronic effects.[24]

For complexes **1** and **2** with dppb and [X = Cl (**1**), NO_3 (**2**)] a broad band is observed with slight modification of the emission energy with the excitation wavelength at 77 K. For compound **3** instead of a broad band, two overlapped bands are observed (Figure S18). The relative intensity of these two bands changes upon modification of the excitation wavelength. Excitation at lower energies increases the intensity of the lower emission energy band. Dual emission upon cooling has been reported for other silver tetracoordinated complexes, attributed to different emissive states which exhibit different distortions from the ground state.[3]

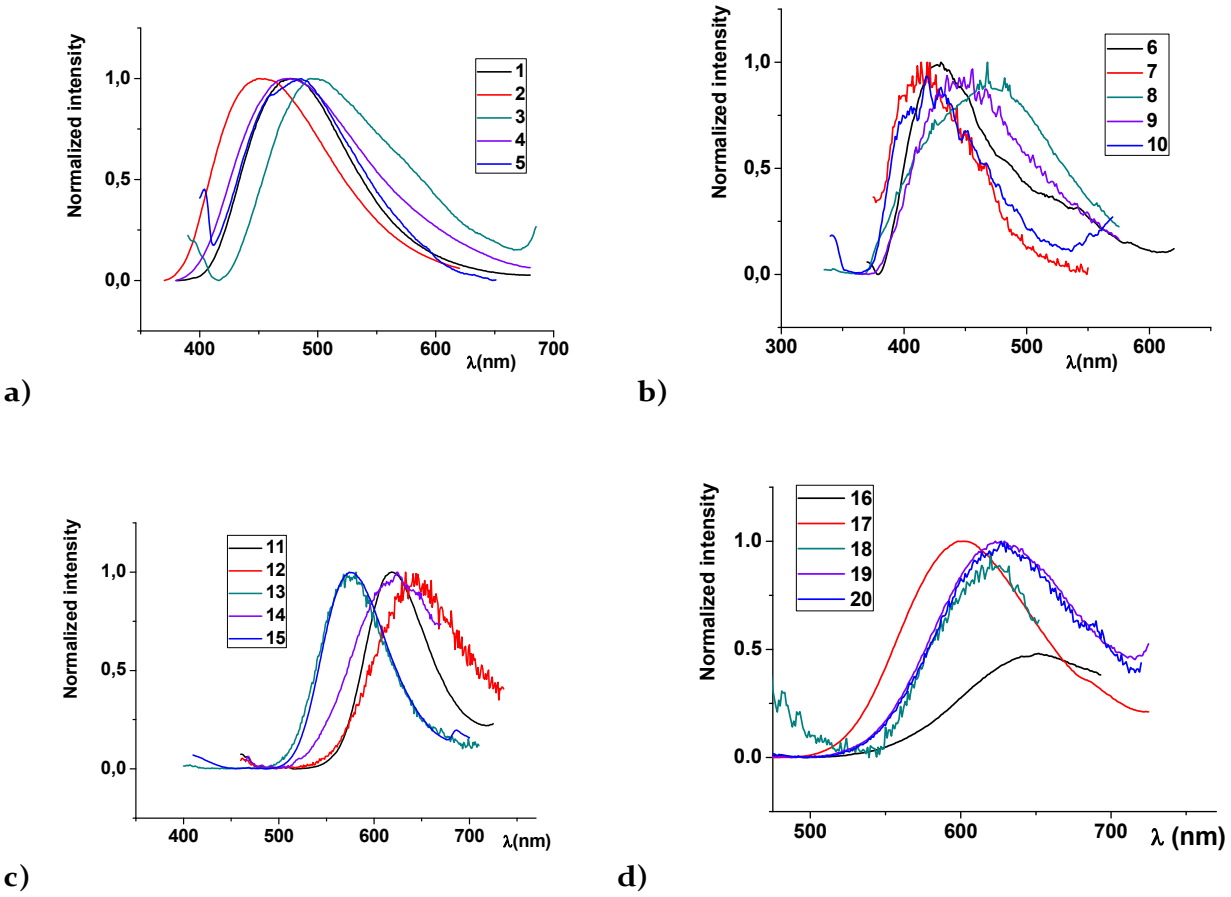

Figure 2. Normalized emission spectra of: a) **1-5**, c) **11-15**, d) **16-20** at room temperature and b) **6-10** at 77 K.

Lifetimes of powder samples at room temperature lie in the microsecond range (5-22 μs) for complexes with dppb and carborane diphosphanes. Those for complexes with xantphos, which are only emissive at low temperature, are in the millisecond range (2.9-5 ms, 77 K). For complex **11** (with dppic) lifetime of 2 μs has been observed at 77 K (15.7 μs at room temperature). Increment of lifetime with temperature would not be consistent with TADF behavior.

Increment of the lifetime at 77 K, compared with that at room temperature, has been proved for compound **5** in the solid state [1270 μs (goodness of fit 0.989) at 85K, 10 μs at room temperature, see Table 1], decrement of lifetime with temperature has been claimed as indicative of TADF.[10,24,25] The observed increment for **5** may be compared with that observed in [Ag(dbp)(dppcc)][16] [1.4 μs (300K), 1300 μs (77K)]. Determination of the energy gap between the S_1 and T_1 states [$\Delta E(S_1-T_1)$], and the decay times of the triplet (T_1) and singlet (S_1) excited states [$\tau(T_1)$ and $\tau(S_1)$, respectively] was carried out for **5** by fitting the observed τ at different temperatures to Equation 1 (K_B = Boltzman constant) using

the least-squares fitting method (Figure 3), leading to the following values $\Delta E(S_1-T_1)$ = 598 cm^{-1}, $\tau(T_1)$ = 0.6 μs, $\tau(S_1)$ = 1.2 ms. Based on these data we propose TADF behavior for complexes **1-5**, but not for complexes with the carborane diphosphanes.

$$\tau = \frac{3+ e^{-\Delta E(S_1-T_1)/K_BT}}{3\left(\frac{1}{\tau(T_1)}\right)+ \left(\frac{1}{\tau(S_1)}\right)e^{-\Delta E(S_1-T_1)/K_BT}} \qquad \text{Equation 1}$$

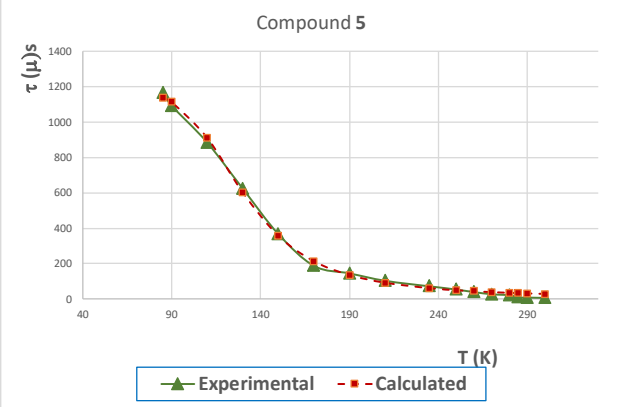

Figure 3. Temperature dependence of the emission lifetime of complex **5** with fitting values using Equation 1.

Influence of the diphosphane: data resumed in Table 1 for complexes with the dppb diphosphane are consistent with the blue-green emissions reported for similar complexes with X = thiolate, bromide and thiocyanate[9,10,15] and dppb or very closed related diphosphanes, despite their dinuclear or mononuclear nature. These facts point out to the conclusion that the anionic ligand and the geometry does not rule the emissive energies of complexes with the dppb diphosphane.

Data of tables 1 and 2 and those above may lead to a more general conclusion: for these systems it seems that is the diphosphane the main factor that governs the emissive properties, including TADF behavior, of the final complexes and not the bridging anion or the nuclearity.

Table 2. Optical measurements for complexes 11-20

P-P / X (compound)		Room T.		τ (μs)[b]	Φ_{PL}[c](%)	K_r[d]	K_{nr}[d]	77 K	
		λEx[a]	λEm[a]					λEx[a]	λEm[a]
dppic / Cl (**11**)	powder	*500 [e]	620	15.7 (1.092)	4	2.5 10^3	6.1 10^4	*510[e]	612
	film	*500 [e]	625	263 (0.972)	4	1.5 10^2	3.6 10^3		
dppic / NO_3 (**12**)	powder	*530 [e]	646	15.0 (1.069)				*430 [e]	625
	film	*450 [e]	584	141.9 (0.965)	11	7.8 10^2	6.3 10^3		
dppic / ClO_4 (**13**)	powder	*500 [e]	576	17.4 (1.085)				346 (sh 392)	555
	film	*300 [e], 376	582	462 (0.981)	27	5.7 10^2	1.5 10^3		
dppic / CF_3COO (**14**)	powder	*500 [e]	624	18.9 (1.039)				360	623
	film	323, 371	603	370 (0.975)	14	3.8 10^2	2.3 10^3		
dppic / CF_3SO_3 (**15**)	powder	*520 [e]	574	14 (1.056)				*450 [e]	567
	film	308, 361	582	531 (0.931)	14	2.6 10^2	1.6 10^3		
dppcc / Cl (**16**)	powder	386	650	0.2 (1.105)				364	646
	film	*450 [e]	644	188 (0.966)	6	3.2 10^2	5.0 10^3		
dppcc / NO_3 (**17**)	powder	365	599	15.7 (1.079)				354	604
	film	*500 [e]	649	214 (0.876)	4	1.9 10^2	4.5 10^3		
dppcc / ClO_4 (**18**)	powder	357	617	18 (1.045)	4	2.2 10^3	5.3 10^4	*400	611
	film	370	618	130 (0.997)	6	4.6 10^2	7.2 10^3		
dppcc / CF_3COO (**19**)	powder	342	626	21 (1.035)				338,393 (sh)	610
	film	376	641	183 (0.992)	5	2.7 10^2	5.2 10^3		
dppcc / CF_3SO_3 (**20**)	powder	368	625	17 (1.005)				339	590
	film	370	625	192 (0.984)	6	3.1 10^2	4.9 10^3		

[a]λEm= emission maximum, λEx= excitation maximum in nm. [b]Lifetimes at room temperature, see also Table S5. [c]Quantum yield at room temperature. [d]From the data at room temperature: calculated radiative constant $k_r = \Phi/\tau$, calculated no radiative constant

$k_{nr} = (1-\Phi)/\tau$. [e]Asterisk (*) before an excitation wavelength means that the band displays maximum values from the beginning of the spectrum until this wavelength.

Calculated K_r for solid samples of complexes with dppb are about 10^4 s^{-1}, higher than those for complexes with caborane diphosphanes (≈ 10^2 s^{-1}). Values of 10^4, 10^5 have been reported for other silver derivatives[15,16,19], although higher values of (10^6, 10^7) have also been reported[17,21].

Luminescence of films of the silver complexes

We have also studied 5 wt% PMMA films of complexes **1-5** and **11-20** at room temperature (Tables 1,2; Figures S19, S20). Except for compound **3**, emission maxima of complexes with dppb (**1-5**) are shifted to the red region, compared with those of powder samples at room temperature. For complexes with carborane diphosphanes (**11-20**)] it is not observed a clear tendency. It has been reported a red shift by changing from solid powder to film, attributed to structural relaxation.[19,24,25] Nevertheless other reports show data that do not follow this trend.[26,27]

Longer lifetimes for PMMA films than those of the corresponding solid powders have been observed. The increment is in general more important for complexes with carborane diphosphanes. As mentioned above, it has been claimed that, as structural relaxation increases, the geometry distortions decrease, resulting a red-shifted emission maximum, and a decreased emission lifetime,[24] but analyzing different reports[16,25,26,27] this trend is not always observed. Thus, it seems that the effects of changing from solid powder to film media in lifetime measurements do not follow a clear tendency.

CIE 1931 color coordinates have been obtained from the emission spectra after removing excitation light (Table S4) and have been represented in the corresponding diagram (Figure 4) which shows the region in which the emissions are observed. The emissions of the complexes span from blue for **2-4**, blue-green for **1**, yellow-orange for **13** and **15** and orange-red for **11**, **12**, **14**, **16-20**. Figure 5 shows photographs of the films of some of the complexes which are consistent with the represented data in Figure 4 and illustrates that the emission of these complexes gives rise to a wide color palette from blue to red through yellow, green and orange.

Quantum yields of films of the blue emissive complexes with dppb (**1-5**) range from 28 to 53%. Higher values have been reported for mononuclear silver complexes with diphosphane and diimine ligands in PMMA[16,17,19,21] but the highest quantum yield values observed for **1-5** are higher than those reported for similar dinuclear complexes with SCN as bridging ligands.[15] For comparison purposes quantum yields of some solids, as representative of the different families of complexes, have been studied (Tables 1 and 2). Those with carborane diphosphanes are similar to that in film. For compound **4** with dppc, quantum yield is lower than the one measured in PMMA film. It has been reported that quantum yields of solid samples are expected to be higher than that in film, due to the expected structural relaxation form crystal to film state.[24] This trend is not always clearly observed[19] or not observed at all.[24,25]

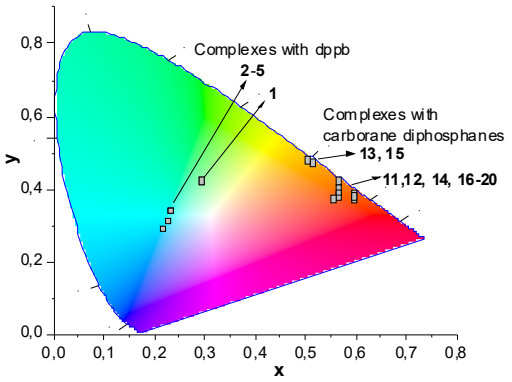

Figure 4. CIE 1931 (angle = 2 degree) diagram of color for complexes with dppb and carborane diphosphanes (see table S4).

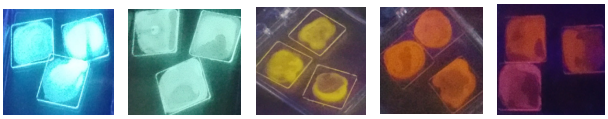

a) b) c) d) e)

Figure 5. Films of complexes **4** (a), **1** (b), **15** (c), **12** (d), **19** (e) in PMMA under UV light.

The presence of a carborane diphosphane in complexes **11-20** leads to an important shift in the emission energy, compared with that of the carborane diphosphane ligands, which is not observed for the other diphosphanes, although the quantum yields are in general lower than those for complexes **1-5** with dppb.

Theoretical studies

Theoretical studies at the TDDFT level were carried out for dinuclear complexes **1** (P-P = dppb, X = Cl), **12** (P-P = dppic, X = NO_3) and **16**, **17**, **20** (P-P = dppcc, X = Cl, NO_3, OTf) and mononuclear complexes [AgBr(xantphos)] and [AgCl(xantphos)] (**6**). The geometries for the S_o state were optimized starting from X-ray data if they were available.

For all the complexes above mentioned, the energy gaps between HOMO/HOMO-1 and LUMO/LUMO+1

present a reasonable agreement with the experimentally obtained excitation energies (Tables S6, S7). Figure 6 illustrates the frontier molecular orbitals data shown in table S6. For all of them, the HOMO and HOMO-1 orbitals are mostly located on silver and phosphorous atoms of the diphosphanes, although for complexes **1** and **16**, with chloride as bridging atom, the anion also participates considerably in the HOMO and HOMO-1 orbitals. Other anions such as NO_3 or OTf do not contribute to these two molecular orbitals.

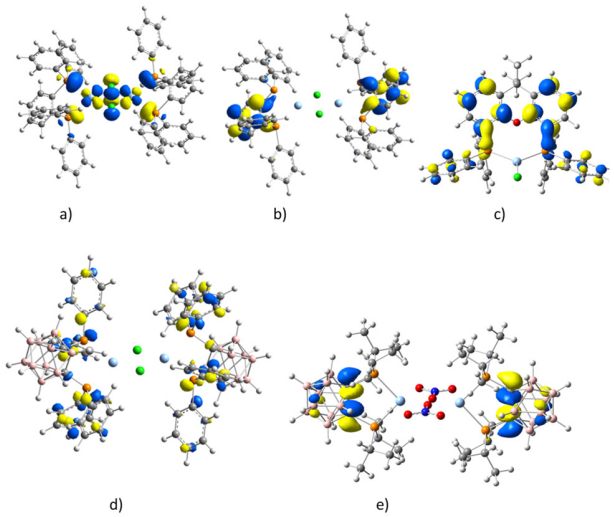

Figure 6. Representative orbitals for complexes: a) HOMO of **1**, b) LUMO+1 of **1**, c) LUMO+1 of **6**, d) LUMO+1 of **16**, e) LUMO+1 of **12**

Different contribution to LUMO and LUMO+1 orbitals are observed depending on the nature of the diphosphane ligand (Figure 6). For complex **1**, bearing the dppb ligand, the LUMO and LUMO+1 are mainly located on the skeleton of the dppb phenyl ring. A similar situation is observed for complexes [AgX(xantphos)] (X = Cl (**6**), Br), their LUMO and LUMO+1 are also found on the aromatic rings of the skeleton of xantphos ligand. A different scenario is found for complexes with the carborane diphosphanes. Hence, for dppcc ligand, the LUMO and LUMO+1 are located on the diphosphane phenyl rings regardless of the bridging ligand X = Cl (**16**), NO_3 (**17**) or OTf (**20**).

For these compounds, the LUMO and LUMO+1 exhibit a dominant π* character. Interestingly, if there is no π system available, as it occurs for complex **12**, where the substituents of the carborane diphosphane are isopropyl groups, the LUMO and LUMO+1 are then located on the C-C bond of the carborane cluster displaying σ* character. It must be taken into account that no π* orbitals from the phosphane substituents are present in dppic.

In order to obtain information about the emission process, geometry optimization of triplet states was carried out. Unfortunately, for dinuclear species they could not be obtained due to very slow convergence or unrealistic bond dissociation channels.

The first excited triplet state was obtained for compounds [AgX(xantphos)] (X = Cl (**6**), Br). Comparison of geometrical parameters between the S_0 and T_1 states shows that Ag-P and Ag-X bond distances are rather similar. These data may be also compared with those reported for the crystal structures of [AgX(xantphos)] (Table S2). Inspection of the deviation of the silver atom from the plane formed by the phosphorous atoms and the X atom reveals that it increases in the excited state for X = Br while it diminishes for X = Cl (Table S8).

It is noticeable the difference between the SOMO+1 orbitals of the T_1 state (Table S9, Figure 7) and the corresponding LUMO orbitals of the S_0 state. In addition to the contributions of phosphorous and skeleton aromatic rings of the xantphos atomic orbitals, which contribute in a major extent to the LUMO orbitals, silver and the halogenide atoms also present some contribution to the SOMO orbitals. Thus, a mixed MLCT and MC nature could be attributed to the $S_0 \leftarrow T_1$ transition in these three coordinated complexes.

The calculated energy gaps $\Delta(S_1\text{-}T_1)$ (Table 3) for complexes [AgX(xantphos)] (X = Cl (**6**), Br) are higher than those reported for other silver derivatives[5,10], but in the range reported for other TADF emissors[1]. It should be taken into account that complexes **6**-**10** are not emissive at room temperature. Complexes with xantphos, although exhibit a small $\Delta(S_1\text{-}T_1)$ energy gap, are not emissive at room temperature, thus TADF at room temperature is not observed.

Table 3. Photophysical data at 77 K and DFT calculated results for [AgX(xantphos)] (X = Cl (6), Br) complexes.

Anion (X)	λ_{EM}[a]	HOMO (a.u.)	LUMO (a.u.)	gap (eV)	T_1 (nm)[b]	$\Delta E(S_1\text{-}T_1)$[c] (Kcal /mol)
Br		-5.29	-1.32	3.97	411.91	4.85
Cl	427	-5.39	-1.30	4.09	414.66	3.15

[a]Experimental emission maximum at 77 K in nm. [b]Calculated emission energy from the excited triplet. [c]$S_1\text{-}T_1$ energy gap calculated for the optimized S_0 structures

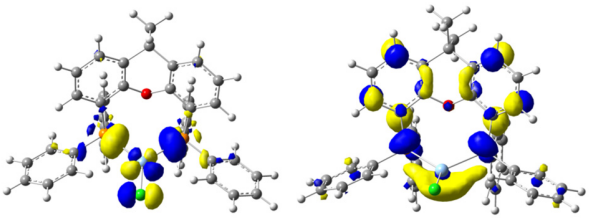

SOMO 170 SOMO+1 171

Figure 7. SOMO orbitals for complex **6**

EXPERIMENTAL

Instrumentation. C, H, N and S analyzes were carried out with a Perkin Elmer 2400 microanalyzer. NMR spectra

were carried out in a Bruker AV 400 or 300 in $CDCl_3$ if solvent is not specified and chemical shifts (ppm) reported relative to the solvent peaks of the deuterated solvent.[28]

Steady-state photoluminescence spectra were recorded with a Jobin-Yvon Horiba Fluorolog FL-3-11. Lifetime measurements were recorded with a Fluoromax phosphorimeter accessory containing a UV xenon flash tube or a Horiba Jobin Ybon LED with pulse duration < 1.2 ns. Frequencies of the LED used were selected according to the excitation energy. Quantum yields were measured by the absolute method using a Hamamatsu Quantaurus-QY C11347 compact one-box absolute quantum yield measurement system. Solid samples were measured using a quartz tube. For film preparation ca. 4 mg of compound and ca. 76 mg of PPMA were solved in 1 mL of CH_2Cl_2 in order to obtain films which contain about 5 wt % of the silver compound. The mixture sonicated for 15 min (if necessary it was previously warmed for seconds). Films were prepared by drop casting of the resulting solution. Two or three films or each complex were prepared and two or three reference samples, each sample was measured using all the reference samples in order to prove the reproducibility of the results.

Crystallography. Crystals suitable for X ray studies were obtained by diffusion of n-hexane over a solution of the corresponding compound in dichloromethane. Crystals of complexes **1** and **17** were mounted in inert oil on a glass fiber and transferred to the cold gas stream of a Xcalibur Oxford Diffraction diffractometer. Data were collected using monochromated Mo Kα radiation (λ = 0.71073 Å). Scan type ω. Absorption correction based on multiple scans were applied with the program SADABS.[29] The structures were refined on F^2 using the program SHELXL-97.[30] All non-hydrogen atoms were refined anisotropically. Hydrogen atoms were included using a riding model. Further details of the data collection and refinement are given in Table S1, which contains the crystallographic data reported in this paper. Cambridge Structure Database 1919976 and 1919977 contains the supplementary crystallographic data for complexes **1** and **17** respectively.

Computational Details. All DFT theoretical calculations have been carried out using the Gaussian program package[31] and the B3LYP functional.[32-34] The calculated vertical excitation energies were obtained by the time-dependent (TD) DFT approach.[35,36] The Karlsruhe def2-SV(P) basis set[37] with additional polarization functions was used on Ag in combination with the Stuttgart effective core potentials, including scalar relativistic effects,[38] for the atoms directly bonded to Ag or bridging ligands the def2-TZVP basis set selected while the def2-SV(P) was used on C, B and H atoms of terminal ligands and non-directly bonded to the metal. All structures were geometrically optimized starting from X-ray structures and the nature of the stationary points has been check by analytical frequency analysis. All calculations were performed without symmetry constraints.

Synthesis and characterization. All reactions were protected from light. Stoichiometric amounts of the corresponding silver salt and diphosphane were mixed in dichloromethane. In order to improve the solubility of the silver salt, for X = ClO_4 and CF_3SO_3, the reactions were carried out in a dichloromethane/diethylether mixture (Scheme 1 and experimental part). Some of these complexes have been previously described, as well as similar complexes with other X bridging atom or diphosphane (see X-ray section). The reported procedures use different solvents [refluxing EtOH, CH_2Cl_2, CH_3CN or not refluxing CH_2Cl_2 (in addition to reference 10 see references 2-7 in S.I.)][10] and in most of the cases reactions are carried out under argon atmosphere. The reported times are between 2 h and 12 h. We have followed a similar procedure to those described with dichloromethane; reactions have been carried out protected from light but at room temperature and no inert atmosphere has been employed, leading to the final compound in shorter times to those reported (ca. 45 min).

CAUTION: Perchlorate salts with organic cations may be explosive. Care should be exercised in using a spatula or stirring rod to mechanically agitate any solid perchlorate.[39,40]

General spectroscopic information. The ^{1}H NMR spectra of complexes **11-20** display a broad resonance between 1-3 ppm in their ^{1}H NMR spectra due to the BH hydrogen atoms of the carborane cage. The resonances corresponding to the methyl groups and CH hydrogen atoms of the diisopropyl substituents of complexes **11-15** appear about 1.3 ppm and 2.4, respectively. Complexes **6-9** display one signal at about 1.6 ppm, corresponding to the methyl groups of the xantphos diphosphane, three signals in the region from 6.5 to 7.3 ppm which correspond to the hydrogen atoms of the xantphos diphosphane and one broad signal corresponding to the hydrogen atoms of the phenyl rings. For some of the complexes the ^{31}P{^{1}H} NMR spectrum at room temperature consists of two doublets corresponding to the coupling of the equivalent phosphorous atoms of the diphosphane to the two silver isotopomers. For the rest of the reported compounds one or two broad signals are observed at room temperature. Splitting of these signals to afford the expected two doublets is only observed at low temperature. For these complexes, the temperature at which the ^{31}P{^{1}H} spectrum has been measured has been included in the experimental part. If no temperature is given the experiment has been carried out at room temperature. The two doublets are centered at about 0 or -7 ppm for complexes with the dppb (**1-5**) or xantphos (**6-10**), respectively. The resonances corresponding to the equivalent phosphorous atoms of the carborane diphosphanes $(PR_2)_2C_2B_{10}H_{10}$ (R = Ph, ^{i}Pr) appear at lower field than those observed for **1-10;** between 11-21 ppm for complexes **11-15** (R = Ph) or 32-36 ppm for complexes **16-20** (R = ^{i}Pr).

Starting materials. The diphosphanes $(PR_2)_2C_2B_{10}H_{10}$ [R = Ph[41] (o-bis(diphenylphosphano)-o-carborane, dppcc);

$^{i}Pr^{42}$ (o-bis(diisopropylphosphano)-o-carborane, dppic)] have been synthesized according to published methods. The diphosphanes dppb (1,2-bis(diphenylphosphano)benzene), xantphos (4,5-bis(diphenylphosphano)-9,9-dimethyl-xanthene) and the silver salts are commercially available and were used without prior treatment.

Complexes [AgX(dppb)] [X = Cl (**1**), NO_3 (**2**), ClO_4 (**3**), CF_3CO_2 (**4**), OTf (**5**)]

A solution of dppb in 10 mL of dichloromethane (0.3 mmol, 133.9 mg) was added to a solution of the silver salt AgX [X = 0.3 mmol; 43.0 mg (X = Cl), 51.0 mg (X = NO_3), 62.2 mg (X = ClO_4), 66.0 mg (X = CF_3CO_2), 77.0 mg (X = CF_3SO_3)] in 10 ml of dichloromethane [reactions with $AgClO_4$ and $Ag(CF_3CO_2)$ were carried out in a mixture dichlorometane/diethyl ether (10/3 mL)]. The mixture stirred for 45 min protected from light. Concentration of the solution *in vacuo* to ca. 5 mL and addition of n-hexane (ca. 10 mL) led to the corresponding solid. **1:** Yield: 73% (129.2 mg). Elemental analysis (%): C 54.3, H 3.63; calculated for $C_{60}H_{48}P_4Ag_2Cl_2 \cdot 2.5\ CH_2Cl_2$ (MW 1391.89) C 53.93, H 3.84. $^{31}P\{^1H\}$ NMR (δ), CD_2Cl_2, -60°C: -0.25 (dd), [$J^{109}Ag$-P = 265.6, $J^{107}Ag$-P = 229.5 Hz]. **2**: Yield: 67% (124.3 mg). Elemental analysis (%): C 57.84, H 3.94, N 2.17; calculated for $C_{60}H_{48}P_4Ag_2N_2O_6\ 1/4CH_2Cl_2$ (MW 1253.91) C 57.71, H 3.91, N 2.24. $^{31}P\{^1H\}$ NMR (δ) $CDCl_3$, -55°C: 0.12 (dd), [$J^{109}Ag$-P = 263.8, $J^{107}Ag$-P = 228.2 Hz]. **3**: Yield: 49% (95.6 mg). Elemental analysis (%): C 52.64, H 3.79; calculated for $C_{60}H_{48}P_4Ag_2Cl_2O_8 \cdot CH_2Cl_2$ (MW 1392.487) C 52.61, H 3.62. $^{31}P\{^1H\}$ NMR (δ): -0.24 (dd), [$J^{109}Ag$-P = 263.1, $J^{107}Ag$-P = 230.6 Hz]. **4**: Yield: 81% (184.6 mg). Elemental analysis (%): C 53.67, H 3.54; calculated for $C_{64}H_{48}P_4Ag_2F_6O_4 \cdot 1.5\ CH_2Cl_2$ (MW 1462.082) C 53.81, H 3.52. $^{31}P\{^1H\}$ NMR (δ) CD_2Cl_2, -55°C: -0.25 (dd), [$J^{109}Ag$-P = 264.6, $J^{107}Ag$-P = 229.5 Hz]. **5**: Yield: 87% (162.0 mg). Elemental analysis (%): C 49.58, H 3.51, S 4.26; calculated for $C_{62}H_{48}P_4Ag_2F_6O_6S_2.1.5CH_2Cl_2$ (MW 1534.19) C 49.71, H 3.35, S 4.18. $^{31}P\{^1H\}$ NMR (δ), CD_2Cl_2, -60°C: -0.29 (dd) [$J^{109}Ag$-P = 264.6, $J^{107}Ag$-P = 228.2 Hz].

Complexes [AgX(xantphos)] [X = Cl (**6**), NO_3 (**7**), ClO_4 (**8**), CF_3CO_2 (**9**), OTf (**10**)]

In a similar procedure to that described above AgX [X = 0.3 mmol; 43.0 mg (X = Cl), 51.0 mg (X = NO_3), 62.2 mg (X = ClO_4), 66.0 mg (X = CF_3CO_2), 77.0 mg (X = CF_3SO_3)] was reacted with xantphos (0.3 mmol, 173.6 mg). **6:** Yield: 70% (150.9 mg). Elemental analysis (%): C 62.96, H 4.38; calculated for $C_{39}H_{32}OP_2AgCl \cdot 1/4\ CH_2Cl_2$ (MW 743.171) C 63.43, H 4.41. $^{31}P\{^1H\}$ NMR (δ): -7.4 (dd), [$J^{109}Ag$-P = 427.3, $J^{107}Ag$-P = 370.7, Hz]. ^1H NMR (δ): 1.67 [s, xantphos-CH_3, 6H], 6.54 [br, xantphos-H, 2H], 7.02 [vt, xantphos-H, 2H, J(HH) = 8 Hz], 7.48 [d (br), xantphos-H, 2H, J(HH) = 8 Hz], 7.18 [m, Ph, 20H]. **7**: Yield: 68% (176.7 mg). Elemental analysis (%): C 60.32, H 4.15, N 1.83; calculated for $C_{39}H_{32}O_4P_2AgN \cdot 0.5CH_2Cl_2$ (MW 790.93) C 59.98, H 4.21, N 1.77. $^{31}P\{^1H\}$ NMR (δ): -6.4 (dd), [$J^{109}Ag$-P = 488.8 Hz, $J^{107}Ag$-P = 423.9 Hz]. ^1H NMR (δ): 1.66 [s, xantphos-CH_3, 6H], 6.65 [m, br, xantphos-H, 2H], 7.11 [vt, xantphos-H, 2H, J(HH) = 8 Hz], 7.57 [dd, xantphos-H, 2H, J(HH) = 4 Hz, J(HH) = 8 Hz], 7.26-7.35 [m, Ph, 20H]. **8**: Yield: 84% (197.9 mg). Elemental analysis (%): C 58.36, H 4.13; calculated for $C_{39}H_{32}O_5P_2AgCl \cdot 1/4CH_2Cl_2$ (MW 807.169) C 58.4, H 4.06. $^{31}P\{^1H\}$ NMR (δ), CD_2Cl_2, -60°C: -7.4 (dd). [$J^{109}Ag$-P = 539.0, $J^{107}Ag$-P = 467.4 Hz]. ^1H NMR (δ): 1.67 [s, xantphos-CH_3, 6H], 6.67 [m, br, xantphos-H, 2H], 7.13 [vt, xantphos-H, 2H, J(HH) = 8 Hz], 7.59 [dd, xantphos-H, 2H, J(HH) = 4 Hz, J(HH) = 8 Hz], 7.26-7.36 [m, Ph, 20H]. **9**: Yield: 79% (202.5 mg). Elemental analysis (%): C 56.53, H 3.69; calculated for $C_{41}H_{32}O_3P_2AgF_3 \cdot CH_2Cl_2$ (MW 884.433) C 57.04, H 3.87. $^{31}P\{^1H\}$ NMR (δ): -7.3 (dd), [$J^{109}Ag$-P = 436.8, $J^{107}Ag$-P = 378.4 Hz]. ^1H NMR (δ): 1.68 [s, xantphos-CH_3, 6H], 6.62 [br, xantphos-H, 2H], 7.10 [vt, xantphos-H, 2H, J(HH) = 8 Hz], 7.56 [dd, xantphos-H, 2H, J(HH) = 8 Hz, J(HH) = 1.4 Hz], 7.34-7.20 [m, Ph, 20H]. **10**: Yield: 81% (189.5 mg). Elemental analysis (%): C 56.51, H 3.96, S 3.92; calculated for $C_{40}H_{32}O_4P_2AgF_3S \cdot 1/4CH_2Cl_2$ (MW 856.788) C 56.42, H 3.82, S 3.7. $^{31}P\{^1H\}$ NMR (δ), CD_2Cl_2, -60°C: -7.2 (dd), [$J^{109}Ag$-P = 525.6, $J^{107}Ag$-P = 455.3 Hz]. ^1H NMR (δ): 1.67 [s, xantphos-CH_3, 6H], 6.67 [m, br, xantphos-H, 2H], 7.13 [vt, xantphos-H, 2H, J(HH) = 8 Hz], 7.59 [dd, xantphos-H, 2H, J(HH) = 4 Hz, J(HH) = 8 Hz], 7.24-7.38 [m, Ph, 20H].

Complexes [AgX{(PR2)2C2B10H10}] [R = ^{i}Pr, X = Cl (**11**), NO_3 (**12**), ClO_4 (**13**), CF_3CO_2 (**14**), OTf (**15**); R = Ph, X = Cl (**16**), NO_3 (**17**), ClO_4 (**18**), CF_3CO_2 (**19**), OTf (**20**)]

In a similar procedure to that described above AgX [X = 0.3 mmol; 43.0 mg (X = Cl), 51.0 mg (X = NO_3), 62.2 mg (X = ClO_4), 66.0 mg (X = CF_3CO_2), 77.0 mg (X = CF_3SO_3)] was reacted with dppcc (0.3 mmol, 153.8 mg) or dppic (0.3 mmol, 113.0 mg). **11**: Yield: 65% (101.7 mg). Elemental analysis (%): C 35.06, H 7.95; calculated for $C_{28}H_{76}B_{20}P_4Ag_2Cl_2 \cdot 1/2$ hexane (MW 1082.74) C 34.39, H 7.73. $^{31}P\{^1H\}$ NMR (δ): 31.7 (dd), [$J^{109}Ag$-P = 341.5, $J^{107}Ag$-P = 296.2 Hz]. ^1H NMR (δ): 1.34 [m, ^{i}Pr-CH_3, 24H], 2.34 [m, ^{i}Pr-CH, 4H], 1-3 [m, br, BH, 10H]. **12**: Yield: 47% (76.2 mg). Elemental analysis (%): C 29.99, H 6.92, N 2.83; calculated for $C_{28}H_{76}B_{20}P_4Ag_2N_2O_6 \cdot 1/2CH_2Cl_2$(MW 1135.27) C 30.15, H 6.83, N 2.47. $^{31}P\{^1H\}$ NMR (δ): 36.3 (dd), [$J^{109}Ag$-P = 344.3, $J^{107}Ag$-P = 396.3 Hz]. ^1H NMR (δ): 1.37 [m, ^{i}Pr-CH_3, 24H], 2.41 [m, ^{i}Pr-CH, 4H], 1-3 [m, br, BH, 10H]. **13**: Yield: 57% (99.2 mg). Elemental analysis (%): C 27.28, H 6.84; calculated for $C_{28}H_{76}B_{20}P_4Ag_2Cl_2O_8$ (MW 1167.65) C 28.8, H 6.56. $^{31}P\{^1H\}$ NMR (δ): 33.8 (dd), [$J^{109}Ag$-P = 388.5, $J^{107}Ag$-P = 340.0 Hz]. ^1H NMR (δ): 1.35 [m, ^{i}Pr-CH_3, 24H], 2.41 [m, ^{i}Pr-CH, 4H], 1-3 [m, br, BH, 10H]. **14**: Yield: 55% (95.6 mg). Elemental analysis (%): C 31.92, H 6.57; calculated for $C_{32}H_{76}B_{20}P_4Ag_2F_6O_4$ (MW 1194.78) C 32.17, H 6.41. $^{31}P\{^1H\}$ NMR (δ): (dd) 35.0, [$J^{109}Ag$-P = 378.8, $J^{107}Ag$-P = 331.8, Hz]. ^1H NMR (δ): 1.33 [m, ^{i}Pr-CH_3, 24H], 2.40 [m, ^{i}Pr-CH, 4H], 1-3 [m, br, BH, 10H]. **15**: Yield: 50% (99.1 mg). Elemental analysis (%): C 27.77, H 6.29, S 6.52; calculated for $C_{30}H_{76}B_{20}P_4Ag_2F_6O_6S_2$ (MW 1266.445) C 28.44, H 6.05, S 5.06. $^{31}P\{^1H\}$ NMR (δ): 34.1 (dd), [$J^{109}Ag$-P = 385.2, $J^{107}Ag$-P = 336.7 Hz]. ^1H NMR (δ): 1.35 [m, ^{i}Pr-CH_3, 24H], 2.39 [m, ^{i}Pr-CH, 4H], 1-3 [m, br, BH, 10H].

16: Yield: 80% (158.1 mg). Elemental analysis (%): C 46.81, H 4.17; calculated for $C_{52}H_{60}B_{20}P_4Ag_2Cl_2 \cdot 1/4CH_2Cl_2$ (MW

1333.02) C 47.08, H 4.57. $^{31}P\{^{1}H\}$ NMR (δ): 10.9 (dd), [J^{109}Ag-P = 337.0, J^{107}Ag-P = 2298.1, Hz]. **17**: Yield: 78% (160.0 mg). Elemental analysis (%): C 41.74, H 3.95, N 2.04; calculated for $C_{52}H_{60}B_{20}P_4Ag_2N_2O_6{\cdot}2\ CH_2Cl_2$ (MW 1534.757) C 42.26, H 4.2, N 1.83. $^{31}P\{^{1}H\}$ NMR (δ), CD_2Cl_2, -70°C: 16.5 (dd), [J^{107}Ag-P = 354.5, J^{109}Ag-P = 410.3 Hz]. **18**: Yield: 87% (188.5 mg). Elemental analysis (%): C 42.64, H 4.17; calculated for $C_{52}H_{60}B_{20}P_4Ag_2Cl_2O_4{\cdot}1.5CH_2Cl_2$ (MW 1503.184) C 42.75, H 4.22. $^{31}P\{^{1}H\}$ NMR (δ), CD_2Cl_2, -60°C: 20.9 (dd), [J^{109}Ag-P = 267.0, J^{107}Ag-P = 230.6 Hz]. **19**: Yield: 81% (163.5 mg). Elemental analysis (%): C 45.36, H 3.92; calculated for $C_{56}H_{60}B_{20}P_4Ag_2F_6O_4$ (MW 1466.91) C 45.85, H 4.12. $^{31}P\{^{1}H\}$ NMR (δ), CD_2Cl_2, -55°C: 17.0 (dd), [J^{109}Ag-P = 395.8 J^{107}Ag-P = 342.3 Hz]. **20**: Yield: 71% (178.4 mg). Elemental analysis (%): C 41.34, H 3.77, S 4.05; calculated for $C_{54}H_{60}B_{20}P_4Ag_2F_6O_6S_2{\cdot}1/2CH_2Cl_2$ (MW 1581.53) C 41.39, H 3.88, S 4.05. $^{31}P\{^{1}H\}$ NMR (δ), CD_2Cl_2, -60°C: 15.3 (dd), [J^{109}Ag-P = 413.9, J^{107}Ag-P = 386 Hz].

CONCLUSIONS

The luminescent properties of complexes $[AgX(P\text{-}P)]_n$ (n = 2, 1) (emission energy, quantum yield or both) are different from those of the free diphosphanes. It is possible to modulate the emission energy of the system $[AgX(P\text{-}P)]_n$ (n = 2, 1) in order to get from blue to red emitters. Changing the diphosphane seems to originate the most important effect, which could determine the observation of TADF emission, whereas modification of the bridging ligand, nuclearity or silver···silver distance seems not to play a relevant role.

Composites of the complexes in PMMA exhibit similar emission energies and higher lifetimes than those of the solid samples. Quantum yields of 5 wt. % PMMA films, among 24 and 53%, have been obtained for the blue emissive films of dppb compounds, for which TADF is proposed and $\Delta E(S_1{-}T_1)$, $\tau(T_1)$ and $\tau(S_1)$ calculated for **5**. The properties of composites of these complexes may be attractive for the design of devices.

Theoretical studies indicate that the HOMO and HOMO-1 are mainly located in the silver atom and the phosphorous atoms of the diphosphanes. The LUMO and LUMO+1 are mainly located in the aromatic skeleton of the dppb or xantphos diphosphane, but in the phenyl rings of the dppcc and in the C-C bond of the carborane cluster for complexes with dppic. Optimization of the first excited triplet state was only possible for [AgX(xantphos)] (X = Cl, Br). In addition to the contributions of phosphorus and skeleton aromatic rings of the xantphos atomic orbitals, which contribute in a major extent to the LUMO orbitals, silver and the halogenide atoms also present some contribution to the SOMO orbitals in these compounds. Thus, a mixed MLCT and MC nature could be attributed to the $S_0{\leftarrow}T_1$ transition in these three coordinated complexes. The $\Delta(S_1\text{-}T_1)$ energy gap lies in the range of that found in complexes for which delayed fluorescence has been proposed, although no TADF is observed at room temperature for these complexes with xantphos.

ASSOCIATED CONTENT

Supporting Information. This material is available free of charge via the Internet at http://pubs.acs.org

-Crystallographic information (CIF) for **1** and **17**.

-Details of the data collection and refinement as well as discussion of the structural data. Additional details of the emissive properties and theoretical studies (PDF).

AUTHOR INFORMATION

Corresponding Author

*Email: ocrespo@unizar.es (O.C.), gimeno@unizar.es (M.C.G.)

Notes

The authors declare no competing financial interest

ACKNOWLEDGMENT

We thank the Ministerio de Economía y Competitividad. (CTQ2016-75816-C2-1-P), PID2019-104379RB-C21 and DGA-FSE (E07_20R) for financial support. We also thank Dr. Rafael Cases Andreu from *Departamento de Fisica de la Materia Condensada, Facultad de Ciencias and Instituto de Ciencia de Materiales de Aragón (ICMA), CSIC–Universidad de Zaragoza (Spain),* for fruitful discussions regarding to lifetime measurements.

REFERENCES

(1) Tao, Y.; Yuan, K.; Chen, T. P.; Xu, T. P.; Li, H.; Chen, R.; C. Zheng, C.; Zhang L.; Huang, W. Thermally Activated Delayed Fluorescene materials Towards the Breakthrough of Organoelectronics. *Adv. Mat.* **2014**, *26*, 7931-7958.

(2) Kaeser, A.; Moudam, O.; Accorsi, G.; Séguy, I.; Navarro, J.; Belbakra, A.; Duhayon, C.; Armaroli, N.; Delavaux-Nicot, B.; Nierengarten, J.-F. Homoleptic Copper(I), Silver(I) and Gold(I) Bisphosphine Complexes. *Eur. J. Inorg. Chem.* **2014**, 1345-1355.

(3) Matsumoto, K.; Shindo, T.; Mukasa, N.; Tsukuda T.; Tsubomura, T. Luminescent Mononuclear Ag(I)-Bis(diphosphine) Complexes: Correlation between the Photophysics and the Structures of Mononuclear Ag(I)-Bis(diphosphine) Complexes. *Inorg. Chem.* **2010**, *49*, 805-814.

(4) Igwa, S.; Hashimoto, M.; Kawata, I.; Hoshino M.; Osawa, M. Photoluminescence Properties, Molecular Structures, and Theoretical Study of Heteroleptic Silver(I) Complexes Containing Diphosphine Ligands. *Inorg. Chem.* **2012**, *51*, 5805-5813.

(5) Owsawa, M.; Kawata, I.; Ishii, R.; Igawa, S.; Hashimoto M.; Hoshino, M. Application of neutral d^{10} coinage metal complexes with an anionic bidentate ligand in delayed fluorescence-type organic light-emitting diodes. *J. Mater. Chem. C* **2013**, *1*, 4375-4383.

(6) Tsukuda, T.; Kawase, M.; Dairiki, A.; K. Matsumoto K.; Tsubomura, T. Brilliant reversible luminescent mechanochromism of silver(I) complexes containing *o*-bis(diphenylphosphino)benzene and phosphinesulphide. *Chem. Commun.* **2010**, *46*, 1905-1907.

(7) Crespo, O.; Gimeno, M.C.; Laguna, A.; R. Marriott, R.; Sáez-Rocher J. M.; Villacampa, M. D. A comparative study of structural patterns and luminescent properties of silver-DAFO complexes with carborane- versus "classical"-diphosphanes. *Dalton Trans.* **2014**, *43*, 12214-12220.

(8) Cui, Y.-Z.; Yuan, Y.; Li, Z.-F.; Liu, M.; Jin, Q.-H.; Jiang, N.; Cui, L.-N.; Gao, S. From ring, chain to network: Synthesis, characterization, luminescent properties of silver(I) complexes constructed by diphosphine ligands and various N-donor ligands. *Polyhedron* **2016**, *112*, 118-129.

(9) Moreno-Alcántar, G.; Nácar-Anaya, A.; Flores-Álamo, M.; Torrens, H.; Luminescent diphosphine fluorophenylthiolate silver(I) compounds that exhibit argentophilic interactions. *N. J. Chem.* **2016**, *40*, 6577-6579.

(10) Osawa, M.; Hashimoto, M.; Kawata, I.; Hoshino, M. Photoluminescence properties of TADF-emitting three-coordinate silver(I) halide complexes with diphosphine ligands: a comparison study with copper(I) complexes. *Dalton Trans.* **2017**, *46*, 12446-12455.

(11) Jin, Q.-H.; Yuan, Y.; Yang, Y.-P.; Qiu, Q.-M.; Liu, M.; Li, Z.-F.; Zhang Z.-W.; Zhang, C.-L. Polynuclear silver(I) complexes of diphosphine ligands and isoquinoline: Synthesis, structural characterization and spectroscopic properties. *Polyhedron* **2015**, *101*, 56–64.

(12) Penney, M. K.; Giang, R.; Burroughs Jr., M. A.; Klausmeyer, K.K. Structure and luminescence of discrete and polymeric Ag(I) complexes formed by the multidentate pyridylphosphine $(PPh_2CH_2)_2N(3\text{-}CH_2C_5H_4N)$. *Polyhedron* **2015**, *87*, 43-54.

(13) Lo, H.-S.; Cheng, E. C.-C.; Xu, H.-L.; Lam, W. H.; Zhu, N.; Au, V. K.-M. Yam, V. W.-W. Synthesis, characterization, photophysics and electrochemistry of hexanuclear silver(I) alkynyl phosphine complexes. *J. Organomet. Chem.* **2016**, *812*, 43-50

(14) Kakizoe, D.; Nishikawa, M.; Degawa T.; Tsubomura, T. Intense blue emission and reversible hypsochromic shift of luminescence caused by grinding based on silver(I) complexes. *Inorg. Chem. Front.* **2016**, *3*, 1381-1387.

(15) Chakkaradhari, G.; Eskelinen, T.; Degbe, C.; Belyaev, A.; Melnikov, A. S.; Grachova, E. V.; Tunik, S. P.; Hirva, P.; Koshevoy, I. O. Oligophosphine-thiocyanate Copper(I) and Silver(I) Complexes and Their Borane Derivatives Showing Delayed Fluorescence. *Inorg. Chem.* **2019**, *58*, 3646–3660.

(16) Shafikov, M. Z.; Suleymanova, A. F.; Czerwieniec, R.; Yersin, H. Design Strategy for Ag(I)-Based Thermally Activated Delayed Fluorescence Reaching an Efficiency Breakthrough. *Chem. Mater.* **2017**, *29*, 1708-1715.

(17) Jia, J.-H.; Liang, D.; Yu, R.; Chen, X.-L.; Meng, L.; Chang, J.-F.; Liao, J.-Z.; Yang, M.; Li, X.-N.; Lu, C.-Z. Coordination-Induced Thermally Activated Delayed Fluorescence: From Non-TADF Donor–Acceptor-Type Ligand to TADF-Active Ag-Based Complexes. *Chem. Mater.* **2020**, *32*, 620–629

(18) Chen, J.; Teng, T.; Kang, L.; Chen, X.-L.; Wu, X.-Y.; Yu, R.; Lu, C.-Z. Highly Efficient Thermally Activated Delayed Fluorescence in Dinuclear Ag(I) Complexes with a Bis-Bidentate Tetraphosphane Bridging Ligand. *Inorg. Chem.* **2016**, 55, 9528–9536.

(19) Shafikov, M. Z.; Suleymanova, A. F.; Czerwieniec, R.; Yersin H. Thermally Activated Delayed Fluorescence from Ag(I) Complexes: A Route to 100% Quantum Yield at Unprecedentedly Short Decay Time. *Inorg. Chem.* **2017**, *56*, 13274–13285

(20) Shafikov, M. Z.; Suleymanova, A. F.; Schinabeck, A.; Yersin, H. Dinuclear Ag(I) Complex Designed for Highly Efficient Thermally. Activated Delayed Fluorescence. *J. Phys. Chem. Lett.* **2018**, *9*, 702–709

(21) Gan, X.-M.; Yu, R.; Chen, X. L.; Yang, M. X.; Lin, L.; Wu, X.-Y.; Lu, C.-Z. A unique tetranuclear Ag(I) complex emitting efficient thermally activated delayed fluorescence with a remarkably short decay time. *Dalton Trans.* **2018**, *47*, 5956–5960.

(22) Li, G.; Ye, H.; Zhu, F.; Yan, G.; Fan, J.; Ma, J.; Adachi, C. Dong, Y.-B. Luminescent Cu(I) and Ag(I) coordination polymers: Fast phosphorescence or thermally activated delayed fluorescence. *Chin. Chem. Lett.* **2019**, *30*, 1931-1934.

(23) Schmidbaur H.; Schier, A. Argentophilic Interactions. *Angew. Chem., Int. Ed. Engl.* **2015**, *54*, 746-784.

(24) Wei, Q.; Zhang, R.; Liu, L.; Zhong, X.-X.; Wang, L.; Li, G.-H.; Li, F.-B.; Alamry, A.; Zhao, Y. From deep blue to green emitting and ultralong fluorescent copper(I) halide complexes containing dimethylthiophene diphosphine and PPh_3 ligands. *Dalton Trans.* **2019**, *48*, 11448-11459.

(25) Mohanjumar, M.; Holler, M.; Meichsner, E.; Nierengarten, J.-F.; Niess, F.; Sauvage, J.-P.; Delavaux-Nicot, B.; Leoni, E.; Monti, F.; Malicka, M.; Cocchi, M.; Bandini, E.; Armaroli, N. Heteroleptic Copper(I) Pseudorotaxanes Incorporating Macrocyclic Phenanthroline Ligands of Different Sizes, *J. Am. Chem. Soc.* **2018**, *140*, 2336-2347.

(26) Xu, L.-J.; Wang, J.-Y.; Xhu, X.-F.; Zeng X.-C.; Chen, Z.-N. *Adv. Funct. Mater.* **2015**, *25*, 3033-3042.

(27) Czerwieniec, Leitl, M.J.; Homeier, H. H. H.; Yersin, H. Cu(I) complexes –Thermally activated delayed fluorescence. Photophysical approach and material design. *Coord. Chem. Rev.* **2016**, *325*, 2-28.

(28) Fulmer, G. R.; Miller, A. J. M.; Sherden, N. H.; Gottlieb, H. E.; Nudelman, A.; Stoltz, B. M.; Bercaw, J. E.; Goldberg K. I. NMR Chemical Shifts of Trace Impurities: Common Laboratory Solvents, Organics, and Gases in Deuterated Solvents Relevant to the Organometallic Chemistry. *Organometallics* **2010**, *29*, 2176-2179.

(29) Bruker SADABS 2.03. Bruker AXS, Inc. Madison, WI, **2000**.

(30) Sheldrick, G. M. SHELXL-97. A program for Crystal Structure Refinement, University of Göttingen, **1977**.

(31) Frisch, M. J.; Trucks, G. W. ; Schlegel, H. B.; Scuseria, G. E.; Robb, M. A.; Cheeseman, J. R.; Scalmani, G.; Barone, V.; Mennucci, B.; Petersson, G. A.; Nakatsuji, H.; Caricato, M.; Li, X.; Hratchian, H. P.; Izmaylov, A. F.; Bloino, J.; Zheng, G.; Sonnenberg, J. L.; Hada, M.; Ehara, M.; Toyota, K.; Fukuda, R.; Hasegawa, J.; Ishida, M.; Nakajima, T.; Honda, Y.; Kitao, O.; Nakai, H.; Vreven, T.; Montgomery Jr, J. A.; Peralta, J. E.; Ogliaro, F.; Bearpark, M.; Heyd, J. J.; Brothers, E.; Kudin, K. N; Staroverov, V. N.; Kobayashi, R.; Normand, J; Raghavachari, K.; Rendell, A.; Burant, J. C.; Iyengar, S. S.; Tomasi, J.; Cossi, M.; Rega, N.; Millam, J. M.; Klene, M.; Knox, J. E.; Cross, J. B.; Bakken, V.; Adamo, C.; Jaramillo, J.; Gomperts, R.; Stratmann, O. Yazyev, R. E. Austin, A. J.; Cammi, R.; Pomelli, C.; Ochterski, J. W.; Martin, R. L.; Morokuma, K.; Zakrzewski, V. G.; Voth, G. A.; Salvador, P.; Dannenberg, J. J.; Dapprich, S.; Daniels, A. D.; Farkas, O.; Foresman, J. B; Ortiz, J. V.; Cioslowski J.; Fox, D. J.; Gaussian, Inc., Wallingford CT, **2013**.

(32) Lee, C.; Yang W.; Parr, R. G. Development of Colle-Salvetti correlation-energy formula into a functional electron density. *Phys. Rev. B.* **1998**, *37*, 785–789.

(33) Becke, A. D. A new mixing of Hartree-fock and local density-functional theories. *J. Chem. Phys.* **1993**, *98*, 1372-1377.

(34) Becke, A. D. Density-functional thermochemistry. III. The role of exact exchange. *J. Chem. Phys.* **1993**, *98*, 5648-5652.

(35) Bauernschmitt, R.; Ahlrichs, R. Treatment of electronic excitations within the adiabatic approximation of time dependent density functional theory. *Chem. Phys. Lett*. **1996**, *256*, 454-464.

(36) Furche, F.; Ahlrichs, R. Adiabatic time-dependent density functional methods for excited state properties. *J. Chem. Phys.* **2004**, *121*, 12772-12773.

(37) Weigend, F.; Ahlrichs, R. Balanced basis sets of split valence, triple zeta valence and quadruple zeta valence quality for H to Rn: Design of assessment of accuracy. *Phys. Chem. Chem. Phys.* **2005**, *7*, 3297-3305.

(38) Dolg, M.; Wedig, U.; Stoll, H.; Preuss, H. Energy-adjusted *ab initio* pseudopotentials for the first row transition elements. *J. Chem. Phys*. **1987**, *86*, 866-872.

(39) Robinson, W. R. Perchlorate salts of metal ion complexes: Potential explosives. *J. Chem. Ed.* ***1985***, *62*, 1001.

(40) "Prudent Practices in the laboratory. Handling and Management", **2011**, p 139. The National Academic Press, Washington D.C.

(41) Alexander R. P.; Schroeder, H. Chemistry of Decaborane-Phosphorus Compounds. IV. Monomeric, Oligomeric, and Cyclic Phosphinocarboranes. *Inorg. Chem.* **1963**, *2*, 1107-1110.

(42) Teixidor, F.; Viñas, C.; Abad, M. M.; Núñez, R.; Kivekäs R.; Sillanpää, R. Procedure for the degradation of 1,2-$(PPh_2)_2$-1,2-dicarba-*closo*-dodecaborane(12) and 1-(PR_2)-2-R′-1,2-dicarba-*closo*-dodecaborane(12). *J. Organomet. Chem.* **1995**, 503, 193-203

Table of contents

SYPNOSIS TOC

Blue to red emissive $[AgX(P\text{-}P)]_n$ (n = 1, 2; X = halogenide or pseudohalogenide; P-P = diphosphane) complexes are reported. Their emissive properties, including TADF, seem to be mostly governed by the selection of the diphosphane and modulated by the auxiliary ligand X. PMMA composites of these complexes display higher quantum yields than those of the free diphosphanes and those with P-P = dppb display the highest values. Optimization of the first excited triplet state for [AgX(xantphos)] (X = Cl, Br) was possible and a mixture of MLCT and MC nature could be attributed to the $S_0 \leftarrow T_1$ transition in these three coordinated complexes.

TOC GRAPHIC